

Remote control of quantum correlations in two-qubit receiver via three-qubit sender

S.I.Doronin and A.I. Zenchuk

*Institute of Problems of Chemical Physics, RAS, Chernogolovka, Moscow reg., 142432,
Russia,*

Abstract

We study the problem of remote control of quantum correlations (discord) in a sub-system of two qubits (receiver) via the parameters of the initial state of another sub-system of three qubits (sender) connected with the receiver by the inhomogeneous spin-1/2 chain. We propose two parameters characterizing the creatable correlations. The first one is the discord between the receiver and the rest of spin-1/2 chain, it concerns the mutual correlations between these two subsystems. The second parameter is the discord between the two nodes of the receiver and describes the correlations inside of the receiver. We study the dependence of these two discords on the inhomogeneity degree of spin chain.

PACS numbers:

I. INTRODUCTION

The problem of controllable remote state creation considered in set of papers [1–5] initiates the problem of creation the states with desirable quantum correlations in a receiver. In particular, the entanglement between the remote qubits is studied in [6, 7], different method of creation of quantum correlations are considered in [8–13].

We shall recall that the problem of remote state control has rather long history starting with the quantum echo [14], which can be referred to as the long distance quantum state transfer. The problem of quantum state transfer itself was formulated in [15]. But even earlier the problem of quantum teleportation was stated [16]. It is worthwhile to give a brief comparison of such closely related branches of quantum communication as quantum teleportation [16–18], quantum state transfer [15, 19–22] and remote quantum state creations [1, 2, 23–25].

The teleportation of the unknown state differs from the two others by the presence of the additional classical communication channel. However, in some sense, this channel is implicitly implemented into the interaction Hamiltonian governing the dynamics of the communication line in the process of state transfer and state creation. The simple analogy can be observed in the perfect state transfer, when the unknown sender’s state moves to the receiver. So, the classical channel as an additional part of the ”communication line” is not needed. Next, the high probability state transfer [26–35] was proposed, which is much simpler realizable in comparison with the perfect state transfer. Besides, instead of transferring the sender’s state itself, we may try to create another state-of-interest directly related with the sender’s state (but different from it) [1, 2, 23–25]. The creation of such states via the spin chain is the subject of ref.[36], where this idea was formulated for the case of mixed sender’s state and short chains. The state creation controlled by the pure sender’s state with one-spin excitation was studied in [37], the similar problem with the physically motivated initial state is considered in [38]. We shall also remark that our algorithm of the quantum state creation develops ideas of the quantum information transfer [39–41] which is an alternative process to the quantum state transfer.

In this paper we consider the remote state-creation in terms of the quantum correlations described by the quantum discord [42–44], which was introduced after the quantum entanglement [45–49]. As quantum correlation parameters, we use the discord between the receiver



FIG. 1: The communication line with three-node sender and two-node receiver

and the rest of spin chain (external correlations) and the discord between the nodes of the receiver (inside correlations). We show their mutual relation and study the map from the control-parameter domain into the two-dimensional space of the mentioned above discords.

The paper is organized as follows. In Sec.II we describe our model of communication line including the Hamiltonian and the initial state. Quantum correlations at the receiver side are considered in Sec.III. The time optimization of the state creation is performed in Sec.IV. Results of the numerical simulation of the creatable correlations in long chains with different inhomogeneity degrees are represented in Sec.V. Conclusions are given in Sec.VI.

II. MODEL OF COMMUNICATION LINE

The communication line considered in our paper is shown in Fig.1. It consists of the three-node sender (the first three nodes of the chain), the two-node receiver (the two last nodes of the chain) and the transmission line connecting them.

A. Interaction Hamiltonian

We consider the evolution governed by the nearest neighbor XY-Hamiltonian

$$H = \sum_{i=1}^{N-1} D_i (I_{ix} I_{(i+1)x} + I_{iy} I_{(i+1)y}), \quad (1)$$

where D_i are the coupling constants between the nearest neighbors, $I_{j\alpha}$ ($j = 1, \dots, N$, $\alpha = x, y, z$) is the j th spin projection on the α -axis. In our model we use the dimensionless time and the following coupling constants:

$$D_i = \frac{\sqrt{N-1} \cos(\phi\pi) + \sin(\phi\pi) \sqrt{i(N-i)}}{\sqrt{N-1} (\cos(\phi\pi) + \sin(\phi\pi))}, \quad 0 \leq \phi \leq \frac{1}{2}. \quad (2)$$

The parameter ϕ in eq.(2) indicates the deviation of our chain from the Ekert one and is referred to as the inhomogeneity parameter. Thus

$$D_i|_{\phi=0} = 1, \quad \text{homogeneous chain}, \quad (3)$$

$$D_i|_{\phi=\frac{1}{2}} = \sqrt{\frac{i(N-i)}{N-1}}, \quad \text{Ekert chain}. \quad (4)$$

Obviously, Hamiltonian (1) commutes with the z -projection of the total spin momentum, $[H, I_z] = 0$. This allows us to significantly simplify the numerical simulations reducing the dimensionality of the Hilbert space in which the spin-dynamics is described. So, working with the one-spin excitation, we use only N -dimensional subspace (of the whole 2^N -dimensional Hilbert space of the N -node spin system) spanned by the following vectors:

$$|n\rangle \equiv |\underbrace{0 \dots 0}_{n-1} 1 \underbrace{0 \dots 0}_{N-n}\rangle, \quad n = 1, \dots, N. \quad (5)$$

B. Initial state of spin chain

We consider the pure one-excitation initial state of the three-node sender of the following general form:

$$|\Psi_0\rangle = \sum_{i=1}^3 a_i |i\rangle, \quad (6)$$

$$\sum_{i=1}^3 |a_i|^2 = 1, \quad (7)$$

where a_i ($i = 1, 2, 3$) are arbitrary parameters with constraint (7). Unlike the initial states considered in [37], our initial state does not involve the ground state $|0\rangle$. According to the Schrödinger equation, the evolution of the pure initial state $|\Psi_0\rangle$ reads:

$$|\Psi(t)\rangle = e^{-iHt} |\Psi_0\rangle. \quad (8)$$

Hereafter we use the following parameterization of the sender's initial state (6) satisfying constraint (7):

$$a_1 = \cos \frac{\alpha_1 \pi}{2} \cos \frac{\alpha_2 \pi}{2}, \quad a_2 = \cos \frac{\alpha_2 \pi}{2} \sin \frac{\alpha_1 \pi}{2} e^{2i\pi\varphi_1}, \quad a_3 = \sin \frac{\alpha_2 \pi}{2} e^{2i\pi\varphi_2}, \quad (9)$$

where

$$0 \leq \alpha_i \leq 1, \quad 0 \leq \varphi_i \leq 1, \quad i = 1, 2, \quad (10)$$

and the parameters $\alpha_i, \varphi_i, i = 1, 2$, are referred to as the control parameters.

C. Local state of receiver

The state of the two-qubit receiver at some time instant t can be obtained reducing the state of the whole chain over spins $1, \dots, N-2$. Written in the basis

$$|0\rangle, |N-1\rangle, |N\rangle, |N(N-1)\rangle, \quad (11)$$

the receiver's density matrix reads as follows:

$$\rho^R \equiv \text{Tr}_{1,2,\dots,N-2}\rho = \begin{pmatrix} 1 - |f_{N-1}|^2 - |f_N|^2 & 0 & 0 & 0 \\ 0 & |f_{N-1}|^2 & f_{N-1}f_N^* & 0 \\ 0 & f_{N-1}^*f_N & |f_N|^2 & 0 \\ 0 & 0 & 0 & 0 \end{pmatrix} \quad (12)$$

(in basis (11), the vector $|N(N-1)\rangle$ means the state with N th and $(N-1)$ th excited spins). Here star means the complex conjugate value and f_{N-1} , f_N , f_0 are the transition amplitudes,

$$f_i = \langle i | e^{-iHt} | \Psi_0 \rangle = R_i e^{2\pi i \Phi_i}, \quad i = 0, \dots, N, \quad (13)$$

where R_i and Φ_i are the real parameters and R_i are positive. Remember the natural constraint

$$|f_N|^2 + |f_{N-1}|^2 \leq 1 \Rightarrow R^2 \equiv R_N^2 + R_{N-1}^2 \leq 1, \quad (14)$$

where the equality corresponds to the perfect two-qubit state transfer because in this case $f_i \equiv 0$ ($i < N-1$).

Obviously, the probability amplitudes appearing in the receiver's state (12) are linear functions of the parameters a_i :

$$f_N(t) = \langle N | e^{-iHt} | \Psi_0 \rangle = \sum_{j=1}^3 a_j \langle N | e^{-iHt} | j \rangle = \sum_{j=1}^3 a_j p_{Nj}(t) \quad (15)$$

$$f_{N-1}(t) = \langle N-1 | e^{-iHt} | \Psi_0 \rangle = \sum_{j=1}^3 a_j \langle N-1 | e^{-iHt} | j \rangle = \sum_{j=1}^3 a_j p_{(N-1)j}(t), \quad (16)$$

where

$$p_{kj}(t) = \langle k | e^{-iHt} | j \rangle = r_{kj}(t) e^{2\pi i \chi_{kj}(t)}, \quad k, j > 0, \quad (17)$$

r_{kj} are the positive amplitudes and $2\pi\chi_{kj}$ ($0 \leq \chi_{kj} \leq 1$) are the phases of p_{kj} . The meaning of p_{kj} is evident. It is the transition amplitude of the excitation from the j th to the k th spin. Emphasize that these amplitudes represent the inherent characteristics of the transmission line and do not depend on the control parameters of the sender's initial state.

III. QUANTUM CORRELATIONS AT RECEIVER SIDE

We introduce two parameters characterizing the quantum correlations at the receiver side. The first of these parameters is the discord Q_{ext} between the receiver and the rest of a chain, it indicates whether these two subsystems correlate to one another. The second one is the discord Q_R between the qubits of the receiver, it characterizes the correlations inside of the receiver.

A. Discord between the receiver and the rest of communication line

Since the initial state of our system is a pure one, it remains pure during the evolution. Thus, the receiver and the rest of communication line compose the whole system in a pure state. Consequently, the discord between these two subsystem is identical to the entanglement between them [8]. The later can be simply calculated in terms of the entropy:

$$Q_{ext} = -\text{Tr} \rho^R \log_2 \rho^R = -\sum_{i=1}^4 \lambda_i \log_2 \lambda_i. \quad (18)$$

In our case, ρ^R (12) is an X -matrix having the following two nonzero eigenvalues:

$$\lambda_1 = 1 - R^2, \quad \lambda_2 = R^2. \quad (19)$$

Consequently,

$$Q_{ext} = -\sum_{i=1}^2 \lambda_i \log_2 \lambda_i = -R^2 \log R^2 - (1 - R^2) \log(1 - R^2). \quad (20)$$

B. Inside discord of the receiver

The formula for discord between the two nodes of receiver is more complicated. For the particular case of X -matrix (12) it was derived in [50] (see Appendix for more details):

$$Q_R = \min(Q_N, Q_{N-1}), \quad (21)$$

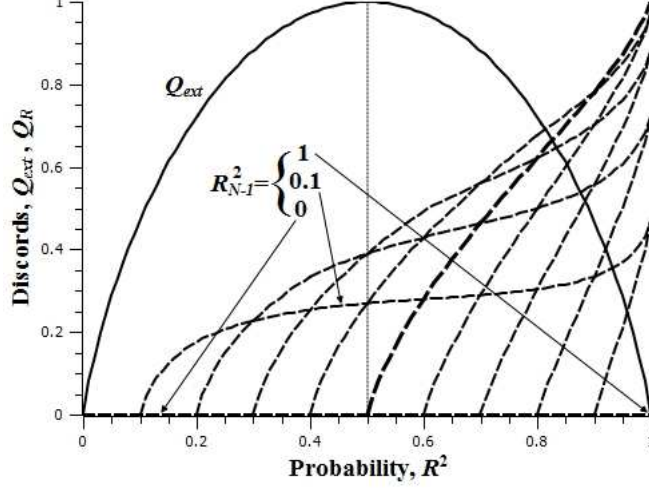


FIG. 2: The discords Q_{ext} (solid line) and Q_R (dash-line) as functions of R^2 and R_{N-1}^2 . The different dash-lines correspond to the different values of $R_{N-1}^2 = 0.1n$, $n = 0, 1, \dots, 10$. The dash-line $R_{N-1}^2 = 0$ coincides with the abscissa axis, the line $R_{N-1}^2 = 1$ shrinks to the point $R^2 = 1$. The bold dash-line corresponds to $R_{N-1}^2 = \frac{1}{2}$, the discord Q_R can take any allowed value on this line, $0 \leq Q_R \leq 1$.

where

$$\begin{aligned}
 Q_N &= 1 - R_{N-1}^2 \log_2 R_{N-1}^2 - \\
 &\quad (1 - R_{N-1}^2) \log_2 (1 - R_{N-1}^2) + R^2 \log_2 R^2 + \\
 &\quad (1 - R^2) \log_2 (1 - R^2) - \\
 &\quad \frac{1}{2} \left(1 - \sqrt{1 - 4R_N^2(1 - R^2)} \right) \log_2 \left(1 - \sqrt{1 - 4R_N^2(1 - R^2)} \right) - \\
 &\quad \frac{1}{2} \left(1 + \sqrt{1 - 4R_N^2(1 - R^2)} \right) \log_2 \left(1 + \sqrt{1 - 4R_N^2(1 - R^2)} \right), \\
 Q_{N-1} &= Q_N|_{N-1 \leftrightarrow N}.
 \end{aligned} \tag{22}$$

This discord depends on the absolute values R_N , R_{N+1} of the transition amplitudes:

C. R - and R_{N-1} -dependence of discords Q_{ext} and Q_R

In Fig.2, we represent the discord Q_{ext} as a function of R^2 (the solid bell-shaped line) and Q_R as a function of R^2 and R_{N-1}^2 (the family of dash-lines, each line corresponds to the particular value of R_{N-1}^2). In this graph we see that the large values of the discord Q_R can be produced by large R . Therewith, the maximal value of the discord Q_R , ($Q_R^{max} = 1$)

corresponds to $R^2 = 1$ and $R_{N-1}^2 = \frac{1}{2}$ (the bold dash-line). On the contrary, the discord Q_{ext} has the maximum at $R^2 = \frac{1}{2}$, this means that Q_R decreases with either $R_{N-1} \rightarrow 0$ or $R_{N-1} \rightarrow 1$. Remark, that there is a region in this figure where Q_R is large while Q_{ext} is rather small (the right upper corner of the figure). In this region the quantum correlations between the receiver and the rest of communication line are minimized and therefore the receiver can be used as (almost) independent object. However, this region is difficult for realization and can be created when the chain is engineered for the high probability state transfer.

IV. TIME OPTIMIZATION OF REMOTE QUANTUM CORRELATIONS

The remote control of quantum states is aimed at creation of required parameters at the receiver side by varying the control parameters. Formally, there is analytical relation between the control parameters and creatable ones. Moreover, the elements of the receiver's density matrix are linear functions of the parameters a_i as was mentioned above. However, the coefficients of these linear functions depend on the transition amplitudes p_{kj} (17) (the t -dependent inherent characteristics of the transmission line) and thus are hardly understandable without graphic representation. Therefore below we numerically study the map of the domain of the two control parameters α_1 and α_2 into the plane of the creatable parameters Q_{ext} and Q_R :

$$(\alpha_1, \alpha_2) \rightarrow (Q_{ext}, Q_R). \quad (23)$$

Note that we set $\varphi_i = 0$ in formulas (9) for a_i because the effect of these phases is negligible in our model, this conclusion was confirmed by the preliminary numerical simulations.

Using the parameter ϕ in eq.(2) we vary the chain from the ideal Ekert chain ($\phi = \frac{1}{2}$, the whole receiver's state-space can be created in terms of Q_{ext} and Q_R in this case) to the homogeneous one ($\phi = 0$, the creatable region is minimal in this case).

A. Time optimization of discords Q_{ext} and Q_R

Taking into account formulas (20) and (21) and the discussion in Sec.III C we conclude that the probability of the state transfer to the receiver side, R^2 , is the most relevant parameter responsible for the quantum correlations and must be studied in more detail.

According to formula (20) the discord Q_{ext} vanishes as either $R = 0$ or $R = 1$. In the ideal case, $R = 1$, the signal is completely collected at the nodes of the receiver. However, usually $R < 1$ and depends on the initial state of the spin system. In the next subsection we perform the time-optimization of R for the initial state (6,9) with the particular values of control parameters: $\alpha_i = 0$, $i = 1, 2$.

1. Time optimization of state transfer probability R^2

The probability R^2 as a function of the time t is an oscillating function of time and reaches the first maximum R_{max}^2 (the largest one) at some time instant t_0 . Both of these parameters (R_{max}^2 and t_0) are shown in Fig.3 as functions of the inhomogeneity parameter ϕ for the chains of different lengths N ,

$$N = 20, 50n, \quad n = 1, \dots, 6. \quad (24)$$

Fig.3a shows that the amplitude approaches unit as $\phi \rightarrow \frac{1}{2}$ (Ekert chain). There is a limiting curve $N \rightarrow \infty$ in Fig.3b (dash-line) showing that the state creation algorithm becomes more N -independent with approaching to the Ekert case, $\phi \rightarrow \frac{1}{2}$, because all curves approach each other in the right upper corner of this figure.

To obtain the approximate form of the limiting curve in Fig.3, we note that each curve in Fig.3a can be approximated by the function

$$F_N = c_N - \exp(-a_N \phi \pi - b_N), \quad (25)$$

with particular values of the coefficients a_N , b_N and c_N (we do not represent these curves in Fig.3a, we also do not give the values of the parameters a_N , b_N and c_N for brevity). Studying the dependence of the parameters a_N , b_N and c_N on N we observe that a_N has the well-formed asymptotics as $N \rightarrow \infty$: $a_\infty \approx 2.232$. The two other parameters b_∞ and c_∞ can be approximated using the "boundary" requirements $F_\infty|_{\phi=\frac{1}{2}} = 1$ and $F_\infty|_{\phi=0} = 0$: $b_\infty \approx -0.03$, $c_\infty \approx 1.031$. Thus, we approximate the limiting curve (the dash-line in Fig.3a) by the function

$$R_\infty = 1.031 - e^{-2.232\phi\pi+0.03}. \quad (26)$$

As for the time instant t_0 , it increases linearly with $N^{\gamma(\phi)}$ ($t \sim N^{\gamma(\phi)}$), where γ decreases with increase in ϕ from $\gamma(0) = 1$ to $\gamma(\frac{1}{2}) = \frac{1}{2}$.

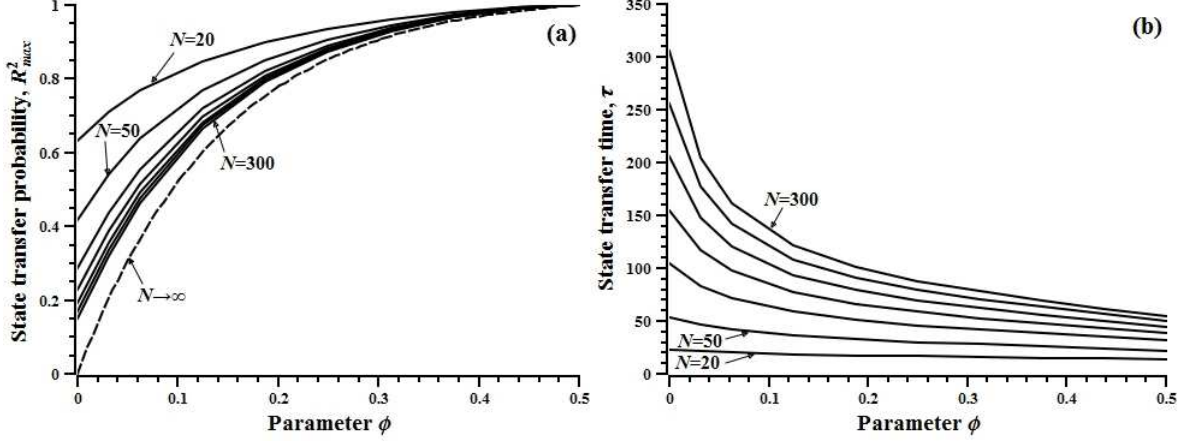


FIG. 3: The maximum of the state transfer probability R^2 and the appropriate time instant τ for the initial state $\Psi_0 = |1\rangle$ and chains of different lengths, $N = 20, 50n$, $n = 1, 2, \dots, 6$.

V. NUMERICAL SIMULATIONS OF MAP (23)

The main purpose of numerical simulation of map (23) is revealing the dependence of the area of creatable region on the inhomogeneity parameter ϕ . In particular, we select the sub-domain in the control-parameter space for which map (23) is (almost) the one-to-one map.

A. Domain of control parameters

For convenience, we separate the whole domain of control parameters (10) into the four sub-domains (we put $\varphi_i = 0$ for the reason indicated above).

The first sub-domain:

$$0 \leq \alpha_i \leq \frac{1}{2}, \quad i = 1, 2. \quad (27)$$

The second sub-domain:

$$\frac{1}{2} \leq \alpha_1 \leq 1, \quad 0 \leq \alpha_2 \leq \frac{1}{2}. \quad (28)$$

The third sub-domain:

$$0 \leq \alpha_1 \leq \frac{1}{2}, \quad \frac{1}{2} \leq \alpha_2 \leq 1. \quad (29)$$

The fourth sub-domain:

$$\frac{1}{2} \leq \alpha_i \leq 1, \quad i = 1, 2. \quad (30)$$

The reasoning for this separation is clarified below in Secs.V B, V C. It will be shown that sub-domain (27) is (almost) one-to-one mapped into the creatable region.

B. Ekert chain

In the limit case of the fully engineered Ekert chain ($\phi = \frac{1}{2}$ in eq.(2)) we are able to cover the whole space of the parameters Q_R , Q_{ext} , see Fig.4 where $N = 20$. In this figure, the horizontal dash-lines correspond to $\alpha_2 = const$, while the solid lines correspond to $\alpha_1 = const$. Emphasize that it is not necessary to work with the whole domain (10) of control parameters because the parameters from the first sub-domain (27) cover the whole creatable space, as is shown in Fig.4a, where some particular values of the control parameters are indicated. Therewith the map (23) is one-to-one map for this sub-domain. The parameters from the second sub-domain (28) are mapped into the same region in Fig.4a (therewith, the parameter α_1 increases from $\frac{1}{2}$ to 1 in passing from the right to the left. We shall point on the third (29) and the fourth (30) sub-domains. Both of them are mapped into the creatable subregion shown in Fig.4b. The indicated values of the control parameters α_i correspond to the third sub-domain (29). The sub-domain (30) maps into the same sub-region with α_1 increasing from $\frac{1}{2}$ to 1 in passing from the right to the left.

Thus, the subregion in Fig.4b is covered four times by the parameters from the all four sub-domains (27-30) and consequently the states from this sub-region are simpler creatable than others. This subregion correspond to the relatively small values of Q_R .

All possible relations between the parameters Q_{ext} and Q_R are realizable in the Ekert case. In particular, the right upper corner in Fig.2 is mapped into the right lower corner in Fig.4.

C. Chains with $\phi < \frac{1}{2}$

Decreasing the parameter ϕ from $\frac{1}{2}$ to 0 we slowly transform the Ekert chain to the homogeneous one. The results of the numerical simulation of map (23) for chains of 20 and

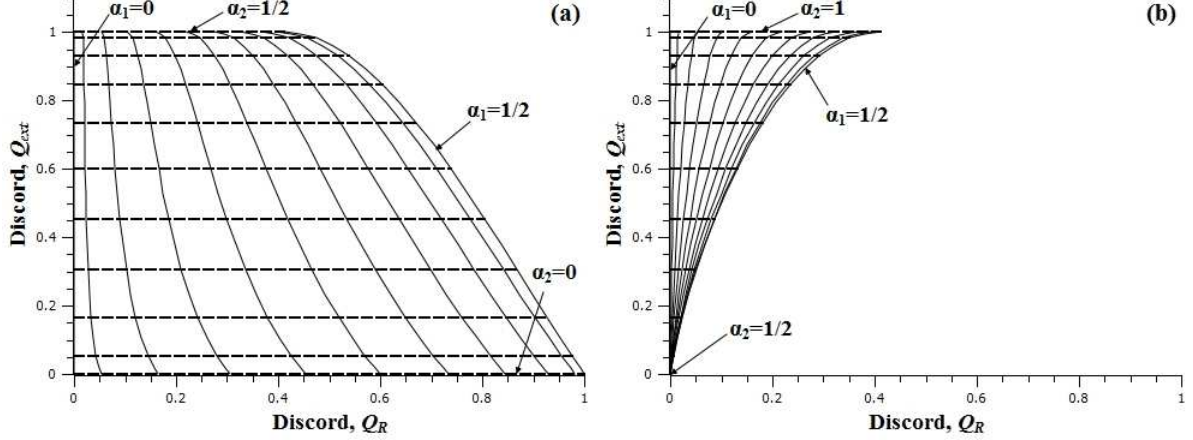


FIG. 4: The discord Q_{ext} verses the discord Q_R for the chain of $N = 20$ nodes with the homogeneity parameter $\phi = \frac{1}{2}$ (Ekert chain) at the time instant $t_0 = 13.69$. The vertical solid lines and the horizon dash-lines correspond to $\alpha_1 = const$ and $\alpha_2 = const$ respectively. The distance between the neighboring lines of each family is 0.05. (a) The control parameters α_i , $i = 1, 2$, from sub-domain (27). Sub-domain of control parameters (28) maps into the same region with α_1 increasing from the right to the left reaching $\alpha_1 = 1$ at the left gridding line (the ordinate axis). (b) The control parameters α_i , $i = 1, 2$, from sub-domain (29) Sub-domain (30) cover the same part of the creatable region with α_1 increasing from the right to the left reaching $\alpha_1 = 1$ at the left gridding line (the ordinate axis).

200 spins and $\phi = \frac{3}{8}, \frac{1}{4}, 0$ are collected in Figs.5 and 6. As was mentioned above, the area of creatable region is minimal in the case of homogeneous chain $\phi = 0$, see Fig.5(c,f) and Fig.6(c,f).

In Figs.5a-b and 6a-b, we depict map (23) corresponding to sub-domain (27) of the control-parameter space, this is almost the one-to-one map. We see that the map in this case can be viewed as a deformation of the Ekert case shown in Fig.4a. Especially this is valid for $\phi = \frac{3}{8}$, see Figs.5a and 6a. In addition, for $\phi = \frac{3}{8}$, we can partially realize the case of large Q_R and small Q_{exp} (the right lower corners in these figures correspond to the right upper corner in Fig.2).

Map (23) of the whole domain of control parameters (10) into the creatable region is depicted in Figs.5d-f and 6d-f for the chains of 20 and 200 spins respectively. In this case the map is far from the one-to-one map with many mutual crossing of the lines inside of the families $\alpha_1 = const$ and $\alpha_2 = const$. We also note that there is a sub-region near the ordinate

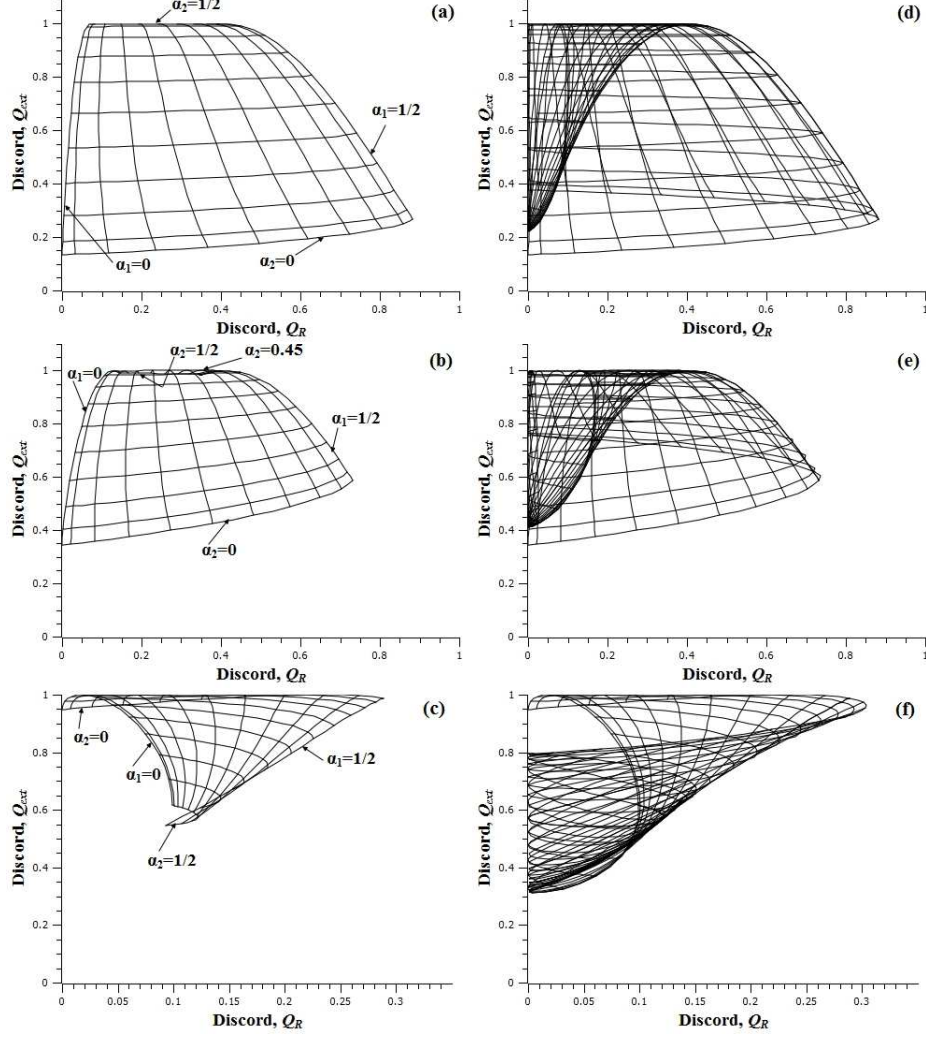


FIG. 5: The discord Q_{ext} verses the discord Q_R for the chain of $N = 20$ nodes. The two crossing families of lines correspond to $\alpha_1 = \text{const}$ and $\alpha_2 = \text{const}$, similar to Fig.4. The interval between the neighboring lines is 0.05 (dimensionless units). (a,b,c) The parameters α_i , $i = 1, 2$ vary inside of sub-domain (27) of parameters α_i , $i = 1, 2$; (d,e,f) The parameters α_i , $i = 1, 2$, vary inside of the whole domain (10). (a,d) $\phi = \frac{3}{8}$, $t_0 = 15.27$, $R_{max}^2 = 0.98$; (b,e) $\phi = \frac{1}{4}$, $t_0 = 16.75$, $R_{max}^2 = 0.94$; (c,f) $\phi = 0$ (homogeneous chain), $t_0 = 22.79$, $R_{max}^2 = 0.63$.

axis (small Q_R) which is covered four times by the parameters from each sub-domain (27-30). Similar to the Ekert case, the states from this sub-region are simpler creatable then states from the other sub-regions covered tree-, two- and one-time.

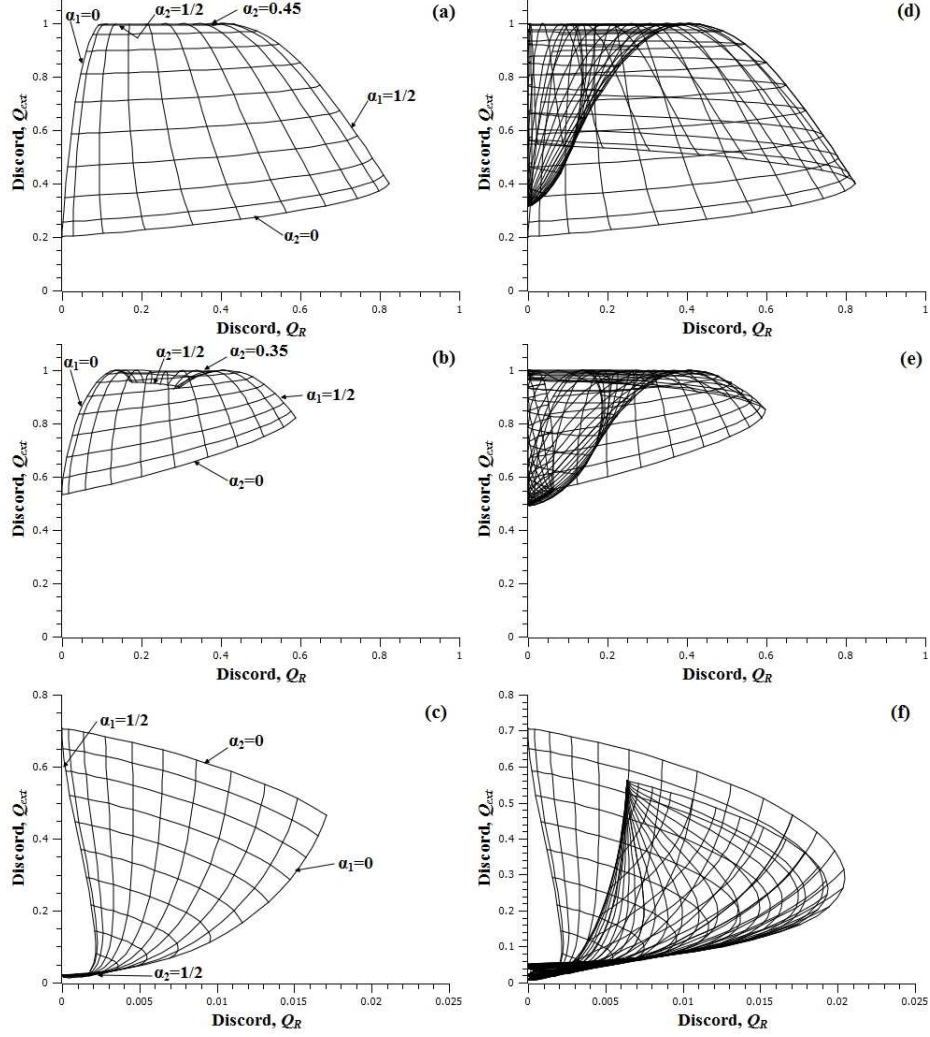


FIG. 6: The same as in Fig.6 for the chain of $N = 200$ nodes. (a,b,c) The parameters α_i , $i = 1, 2$, vary inside of sub-domain (27); (d,e,f) The parameters α_i , $i = 1, 2$, vary inside of the whole domain (10). (a,d) $\phi = \frac{3}{8}$, $t_0 = 55.91$, $R_{max}^2 = 0.97$; (b,e) $\phi = \frac{1}{4}$, $t_0 = 69.48$, $R_{max}^2 = 0.88$; (c,f) $\phi = 0$ (homogeneous chain), $t_0 = 205.54$, $R_{max}^2 = 0.19$.

VI. CONCLUSIONS

In this work we study the possibility of remote creation of quantum correlated states. We consider the model with the nearest neighbor XY-Hamiltonian and the coupling constants depending on the parameter ϕ characterizing the inhomogeneity of the chain. At that, the homogeneous chain corresponds to $\phi = 0$, while the Ekert chain corresponds to $\phi = \frac{1}{2}$. We consider the two parameters characterizing quantum correlations. The first one, Q_{ext} , is the discord between the receiver and the rest of communication line, it shows whether

the receiver is independent on other spins of the chain. The second parameter, Q_R , is the discord between the two nodes of the receiver and characterizes correlations inside of the receiver. We show that the creatable region increases with an increase in the parameter ϕ , so that the complete state-space in terms of the parameters Q_{ext}, Q_R can be covered in the case $\phi = \frac{1}{2}$ (Ekert chain). With decrease in ϕ , the creatable region reduces covering the minimal area at $\phi = 0$ (homogeneous chain). If $\phi = \frac{3}{8}$ (i.e. the almost Ekert chain), the creatable region does not significantly reduces as can be seen in Figs.5a,d and 6a,d. Moreover, comparing Fig.5a with Fig.6a allows us to conclude that, in this case, the area of creatable region slightly depends on N , which agrees with the prediction of Sec.IV A 1. However, decreasing ϕ , we observe that the area of creatable region reduces with increase in N , which is especially evident from the comparison of Fig.5c(f) with Fig.6c(f). The most interesting case corresponds to the right upper corner in Fig.2a, where Q_R reaches large values while Q_{ext} is significantly less. In this case the quantum correlations between the receiver and the rest spins of communication line are minimal, so that the receiver can be considered as an independent subsystem. The states from this corner can be created in the chains engineered for the high probability state transfer (see the right lower corners in Fig.4 (Ekert chain) and in Figs.5a,d and 6a,d, where $\phi = \frac{3}{8}$).

We also emphasize that there is a domain in the control parameter space (27) which almost uniquely covers a large part of the creatable region, as shown in Figs.5a-c and 6a-c. Outside of this domain the map loses its uniqueness, see Figs.5d-f and 6d-f. In these figures, we also see that the subregion near the ordinate axis (Q_R is relatively small) is covered four times by the control parameters and thus it is simpler for realization in comparison with other subregions.

It is interesting that the inhomogeneity in our model establishes the lower limit on the state-transfer probability R^2 which is estimated by the empirically obtained dash-curve in Fig.3.

This work is partially supported by the program of RAS "Element base of quantum computers", project "Quantum registers on the virtual particles (fermions) in one-dimensional chains of interacting nuclear spins in the external magnetic field", by the Russian Foundation for Basic Research, grants No.15-07-07928. A.I.Z. is partially supported by DAAD (the Funding program "Research Stays for University Academics and Scientists", 2015 (50015559)).

VII. APPENDIX. DISCORD BETWEEN TWO NODES OF RECEIVER

We call Q_{N-1} and Q_N discords calculated using the measurements over the $(N-1)$ th and N th nodes respectively. First, we obtain the formula for Q_N :

$$Q_N = \mathcal{I}(\rho) - \mathcal{C}^N(\rho). \quad (31)$$

Here $\mathcal{I}(\rho)$ is the total mutual information [43] which may be written as follows:

$$\mathcal{I}(\rho) = S(\rho^{(N-1)}) + S(\rho^{(N)}) + \sum_{j=0}^1 \lambda_j \log_2 \lambda_j, \quad (32)$$

where λ_j ($j = 0, 1$) are the non-zero eigenvalues of the density matrix ρ^R (12),

$$\lambda_0 = \rho_{NN} + \rho_{(N-1)(N-1)}, \quad \lambda_1 = 1 - \lambda_0. \quad (33)$$

Here ρ_{ij} are the elements of the matrix ρ^R ($\rho_{NN} = |f_N|^2$, $\rho_{(N-1)(N-1)} = |f_{N-1}|^2$), $\rho^{(N-1)} = \text{Tr}_N \rho^R$ and $\rho^{(N)} = \text{Tr}_{N-1} \rho^R$ are the reduced density matrices, the entropies $S(\rho^{(N-1)})$ and $S(\rho^{(N)})$ are given by the following formulas:

$$S(\rho^{(N-1)}) = -(1 - \rho_{NN}) \log_2(1 - \rho_{NN}) - \rho_{NN} \log_2 \rho_{NN}, \quad (34)$$

$$S(\rho^{(N)}) = -(1 - \rho_{(N-1)(N-1)}) \log_2(1 - \rho_{(N-1)(N-1)}) - \rho_{(N-1)(N-1)} \log_2 \rho_{(N-1)(N-1)}.$$

The so-called classical counterpart $\mathcal{C}^B(\rho^R)$ of the mutual information can be found considering the minimization over the projective measurements performed over the N th spin [51]:

$$\mathcal{C}^{(N)}(\rho) = S(\rho^{(N-1)}) - \min_{\eta \in [0,1]} (p_0 S_0 + p_1 S_1), \quad (35)$$

where

$$S(\theta_i) \equiv S_i = -\frac{1 - \theta_i}{2} \log_2 \frac{1 - \theta_i}{2} - \frac{1 + \theta_i}{2} \log_2 \frac{1 + \theta_i}{2}, \quad (36)$$

$$p_i = \frac{1}{2} \left(1 + (-1)^i \eta (1 - 2\rho_{(N-1)(N-1)}) \right), \quad (37)$$

$$\theta_i = \frac{1}{p_i} \left[(1 - \eta^2) \rho_{(N-1)(N-1)} \rho_{NN} + \right. \quad (38)$$

$$\left. \frac{1}{4} \left(1 - 2\rho_{NN} + (-1)^i \eta (1 - 2(\rho_{(N-1)(N-1)} + \rho_{NN})) \right)^2 \right]^{1/2},$$

$$i = 0, 1.$$

Here we introduce the parameter η instead of k in [51] ($k = (1 + \eta)/2$). It is simple to show that the quantum discord Q_{N-1} obtained performing the von Neumann type measurements on the particle $N - 1$ can be calculated as follows:

$$Q_{N-1} = Q_N|_{\rho_{(N-1)(N-1)} \leftrightarrow \rho_{NN}}. \quad (39)$$

Then we define the discord Q_R as the minimum of Q_{N-1} and Q_N [52], see eq.(21). One can show [50] that the minimum in eq.(35) corresponds to $\eta = 0$ so that we result in the explicit formulas (21) (22) for the discord Q_R .

-
- [1] N.A.Peters, J.T.Barreiro, M.E.Goggin, T.-C.Wei, and P.G.Kwiat, Phys.Rev.Lett. **94**, 150502 (2005)
 - [2] N.A.Peters, J.T.Barreiro, M.E.Goggin, T.-C.Wei, and P.G.Kwiat in *Quantum Communications and Quantum Imaging III*, ed. R.E.Meyers, Ya.Shih, Proc. of SPIE **5893** (SPIE, Bellingham, WA, 2005)
 - [3] B.Dakic, Ya.O.Lipp, X.Ma, M.Ringbauer, S.Kropatschek, S.Barz, T.Paterek, V.Vedral, A.Zeilinger, C.Brukner, and P.Walther, Nat. Phys. **8**, 666 (2012).
 - [4] G.Y. Xiang, J.Li, B.Yu, and G.C.Guo Phys. Rev. A **72**, 012315 (2005)
 - [5] S.Pouyandeh, F. Shahbazi, A. Bayat, Phys.Rev.A **90**, 012337 (2014)
 - [6] L.Banchi, A. Bayat, P. Verrucchi, and S.Bose, Phys.Rev.Let. **106**, 140501 (2011)
 - [7] B. Chen and Zh. Song, Sci. China-Phys., Mech.Astron. **53**, 1266 (2010).
 - [8] A.Datta, A.Shaji, C.M.Caves, Phys.Rev.Lett. **100**, 050502 (2008)
 - [9] B.P.Lanyon, M.Barbieri, M.P.Almeida, A.G.White, Phys.Rev.Lett. **101**, 200501 (2008)
 - [10] W.J.Nie, Yu.H.Lan, Yo.Li, and Sh.Ya.Zhu, Sci.China-Phys., Mech. Astron **57**, 2276 (2014)
 - [11] P. Zhang, B. You, and L.-X. Cen, Chin. Sci. Bull., **59**, 3841 (2014)
 - [12] J.X. Sci, W. Xu, G. Sun et al, Chin. Sci. Bull. **59**, 2547 (2014)
 - [13] S. Rodriques, N. Datta, and P. J. Love, Phys. Rev. A **90**, 012340 (2014)
 - [14] E.B.Fel'dman, R.Brüschweiler and R.R.Ernst, Chem.Phys.Lett. **294**, 297 (1998)
 - [15] S. Bose, Phys. Rev. Lett. **91**, 207901 (2003)
 - [16] C.H.Bennett, G.Brassard, C.Crépeau, R.Jozsa, A.Peres, and W.K.Wootters, Phys. Rev. Lett. **70**, 1895 (1993)

- [17] D.Bouwmeester, J.-W. Pan, K.Mattle, M.Eibl, H.Weinfurter, and A. Zeilinger, *Nature* **390**, 575 (1997)
- [18] D. Boschi, S. Branca, F. De Martini, L. Hardy, and S. Popescu, *Phys. Rev. Lett.* **80**, 1121 (1998)
- [19] M.Christandl, N.Datta, A.Ekert and A.J.Landahl, *Phys.Rev.Lett.* **92**, 187902 (2004)
- [20] C.Albanese, M.Christandl, N.Datta and A.Ekert, *Phys.Rev.Lett.* **93**, 230502 (2004)
- [21] P.Karbach and J.Stolze, *Phys.Rev.A* **72**, 030301(R) (2005)
- [22] G.Gualdi, V.Kostak, I.Marzoli and P.Tombesi, *Phys.Rev. A* **78**, 022325 (2008)
- [23] C.H.Bennett, D.P.DiVincenzo, P.W.Shor, J.A.Smolín, B.M.Terhal, and W.K.Wootters, *Phys.Rev.Lett.* **87**, 077902 (2001); Erratum, C.H.Bennett, D.P.DiVincenzo, P.W.Shor, J.A.Smolín, B.M.Terhal, and W.K.Wootters, *Phys. Rev. Lett.* **88**, 099902(E) (2002)
- [24] C.H.Bennett, P.Hayden, D.W.Leung, P.W.Shor, and A.Winter, *IEEE Transectction on Information Theory* **51**, 56 (2005)
- [25] G.L.Giorgi, *Phys. Rev. A* **88**, 022315 (2013)
- [26] E.I.Kuznetsova and A.I.Zenchuk, *Phys.Lett.A* **372**, pp.6134-6140 (2008)
- [27] J.Stolze, G. A. Álvarez, O. Osenda, A. Zwick in *Quantum State Transfer and Network Engineering. Quantum Science and Technology*, ed. by G.M.Nikolopoulos and I.Jex, Springer Berlin Heidelberg, Berlin, p.149 (2014)
- [28] A. Bayat and V. Karimipour *Phys.Rev.A* **71**, 042330 (2005)
- [29] P. Cappelaro, *Phys.Rev.A* **83**, 032304 (2011)
- [30] W. Qin, Ch. Wang, G. L. Long, *Phys.Rev.A* **87**, 012339 (2013)
- [31] A.Bayat, *Phys. Rev. A* **89**, 062302 (2014)
- [32] C. Godsil, S. Kirkland, S. Severini, Ja. Smith *Phys. Rev. Lett.* **109**, 050502 (2012)
- [33] R.Sousa, Ya. Omar, *New J. Phys.* **16**, 123003 (2014).
- [34] D. Burgarth and S. Bose, *Phys.Rev.A* **71**, 052315 (2005)
- [35] K. Shizume, K. Jacobs, D. Burgarth, and S. Bose, *Phys. Rev. A* **75**, 062328 (2007)
- [36] A.I.Zenchuk, *Phys. Rev. A* **90**, 052302(13) (2014)
- [37] G. A. Bochkin and A. I. Zenchuk, *Phys.Rev.A* **91**, 062326(11) (2015)
- [38] E.B. Fel'dman, E.I. Kuznetsova, A.I. Zenchuk, arXiv:1507.07738
- [39] S.Yang, A. Bayat, S. Bose, *Phys.Rev.A* **84**, 020302 (2011)
- [40] A.I.Zenchuk, *J. Phys. A: Math. Theor.* **45** (2012) 115306

- [41] S. Pouyandeh, F. Shahbazi, Int. J. Quantum Inform. **13**, 1550030 (2015)
- [42] L. Henderson, V. Vedral, J. Phys. A: Math. Gen. **34**, 6899 (2001)
- [43] H.Ollivier and W.H.Zurek, Phys.Rev.Lett. **88**, 017901 (2001)
- [44] W.H. Zurek, Rev. Mod. Phys. **75**, 715 (2003)
- [45] W.K. Wootters,, Phys. Rev. Lett. **80**, 2245 (1998)
- [46] S.Hill and W.K.Wootters, Phys. Rev. Lett. **78**, 5022 (1997)
- [47] A.Peres, Phys. Rev. Lett. **77**, 1413 (1996)
- [48] L.Amico, R.Fazio, A.Osterloh and V.Ventral, Rev. Mod. Phys. **80**, 517 (2008)
- [49] R.Horodecki, P.Horodecki, M.Horodecki and K.Horodecki, Rev. Mod. Phys. **81**, 865 (2009)
- [50] E. B. Fel'dman and A. I. Zenchuk, Quantum Inf. Process., **13** (2014) 201
- [51] M.Ali, A.R.P.Rau, G.Alber, Phys.Rev.A **81**, 042105 (2010); Erratum: Phys.Rev.A **82**, 069902(E) (2010)
- [52] E.B.Fel'dman and A.I.Zenchuk, Phys. Lett. A **373** (2009) 1719